DESIGN AND EXPERIMENT OF INDEPENDENT FOUR-WHEEL DRIVE SYSTEM FOR ELECTRIC VEHICLES

Pham Quoc Phong[1]*, Huynh Dung Liem[2], Duong Van Kien[2]

[1]*College of Engineering and Technology, Tra Vinh University, Vietnam*
[2]*Faculty of Automotive Engineering Technology, Nam Can Tho University, Vietnam*

*Corresponding author: phongpham@tvu.edu.vn

(Received: November 07, 2025; Revised: January 08, 2026; Accepted: January 13, 2026)

DOI: 10.31130/ud-jst.2026.24(1).616E

Abstract - This paper presents the design and experimental implementation of an independent Four-Wheel Drive (4WD) system for a low-speed electric vehicle, using four 350 W Brushless DC (BLDC) hub motors integrated directly into the wheels. Each motor is independently controlled by a PID controller and an Arduino Mega 2560 microcontroller, allowing precise speed regulation of each wheel. The speed feedback signals are obtained from the Hall sensors integrated within the motors, while the steering angle Encoder sensor and Hall-type throttle pedal sensor provide input data for calculating the reference speed of each wheel. Experimental results show that the PID controller implemented on the Arduino Mega 2560 is capable of effectively controlling the speed of all four wheels, ensuring stable vehicle operation. Although minor speed fluctuations occur due to load differences, the system responds well when transitioning from low to high speeds.

Key words - Arduino; BLDC; Electric vehicle; Independent Four-Wheel Drive; PID

1. Introduction

Electric vehicles (EVs) are gaining increasing attention due to their widespread application in freight transportation, travel, and low-speed environments such as tourist areas and internal roads. For small-sized, low-speed electric vehicles, long operating time and compact packaging are important requirements. However, conventional drivetrains with mechanical differentials take up significant space, limiting battery capacity and the installation of auxiliary equipment. To overcome this limitation, an independent four-wheel-drive (4WD) system based on distributed drive technology has been proposed, eliminating bulky mechanical components such as gearboxes, drive shafts, and mechanical differentials, thereby simplifying the chassis structure and improving space utilization [1]. In this architecture, each wheel is driven independently by a brushless DC (BLDC) motor, which allows electronic speed control to completely replace the mechanical differential.

Motor speed regulation using proportional–integral–derivative (PID) controllers has been recognized as an effective approach owing to its simplicity, high reliability, and stable performance under diverse operating conditions [4], [5]. Wang [6] demonstrated that implementing PID controllers in BLDC motor drive systems enhances stability and load response. Several studies have demonstrated the effectiveness of electronic differential systems based on the Ackermann steering principle for independent wheel control, achieving accurate speed distribution, stable transient response, and improving vehicle maneuverability [7]–[12]. In 2024, Yıldırım et al. [13] designed and implemented an electronic differential system for electric vehicles using four PMSM motors mounted in wheels, based on the Ackermann–Jeantand kinematic model. The simulation and experimental results show that the system operates stably, safely and ensures the reliable operation of all-wheel drive.

Based on previous studies, the development of 4WD system using BLDC motors with PID control for low-speed EVs is considered technically feasible. A speed control model for such a 4WD system is therefore proposed for practical applications in speed-restricted environments, small speed fluctuations may arise due to load variations between individual wheels, but the proposed control is expected to provide satisfactory speed tracking performance switching between operating conditions.

2. Modeling development

2.1. Independent four-wheel drive system

4WD system for the electric vehicle is installed on a small-scale, single-seat EV test frame, as illustrated in Figure 1. The vehicle frame employs a simplified chassis design to focus primarily on evaluating the performance of the drive system. Dimension of the model as follows: a wheelbase of 1,350 mm, a track width of 890 mm, a ground clearance of 460 mm, and a wheel diameter of 356 mm. 4WD in EV must overcome various types of resistive forces during motion. The total traction force (F_k) that the motors need to generate is the sum of these resistive forces:

$$F_k = F_i + F_f + F_w + F_j \quad (1)$$

The aerodynamic drag F_w is the force exerted by air on the vehicle and can be expressed as:

$$F_w = \frac{C_D A v^2}{21.15} \quad (2)$$

The rolling resistance F_f encountered by the vehicle during motion can be calculated as:

$$F_f = mgf_r \cos\alpha \quad (3)$$

The grade resistance F_i is calculated as:

$$F_i = mg \sin\alpha \quad (4)$$

The inertial resistance corresponding F_j is given by:

$$F_j = \sigma m \frac{dv}{dt} \tag{5}$$

By substituting equations (2), (3), (4), and (5) into equation (1), we obtain:

$$F_k = mg\sin\alpha + mgf_r\cos\alpha + \frac{C_D A v^2}{21.15} + \sigma m\frac{dv}{dt} \tag{6}$$

The required power of the entire system (P_{max}) can be calculated as:

$$P_{\max} = F_k \times V_{\max} \tag{7}$$

The power required for each motor (P_{motor}) is:

$$P_{motor} = \frac{P_{\max}}{4} \tag{8}$$

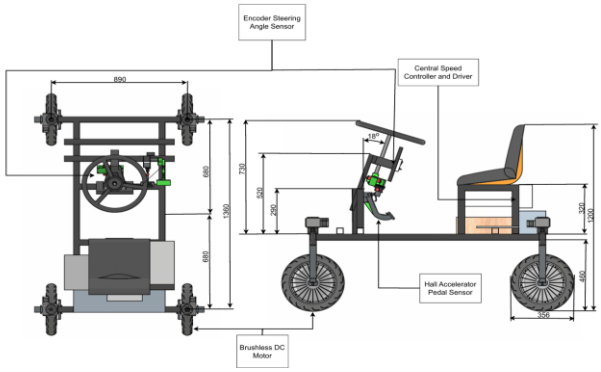

Figure 1. *Layout of the independent four-wheel drive system*

Table 1. *Motor selection parameters*

Description	Symbol	Value
Total vehicle mass	m	200 kg
Gravitational acceleration	g	9.81 m/s²
Rolling resistance coefficient	f_r	0.015
Road slope angle	α	5°
Aerodynamic drag coefficient	C_D	0.8
Vehicle frontal area	A	0.9 m²
Maximum vehicle speed	V_{max}	15 km/h
Rotational mass factor	σ	1.05
Longitudinal acceleration	$\frac{dv}{dt}$	0.5 m/s²

According to Table 1 specifications, the required power for each motor is approximately 326 W. Therefore, a 36V–350W BLDC motor is used for test terrain conditions. The four BLDC motors are mounted directly within the wheels. BLDC motor consists of a rotor with permanent magnets, a three-phase wound stator, and a Hall sensor providing 26 pulses per revolution to determine rotor position for control while simultaneously sending the motor rotation count to the controller. Each wheel is equipped with an individual driver.

The steering system employs a 400-pulse-per-revolution optical encoder, transmitting channel A and B signals to an Arduino microcontroller to determine the rotation direction and steering angle within ±35°, facilitating wheel speed adjustments. The accelerator pedal uses a contactless Hall sensor, producing a voltage signal ranging from 1.1 V to 4.8 V, corresponding to vehicle speeds of 0~4.17 m/s (0~15 km/h). This signal is sent to the controller, ensuring rapid and precise response to driver input.

2.2. Ackermann model

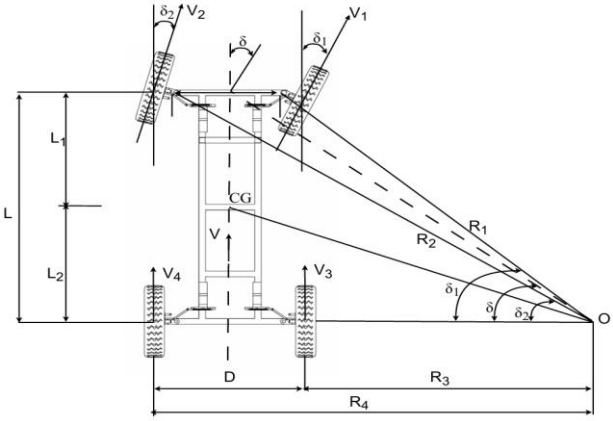

Figure 2. *Model for an independent four-wheel drive electric vehicle*

The model depicted in Figure 2, four wheels rotate an instantaneous center (O) during a turn. The instantaneous center O is precisely determined by the vehicle's steering angle (δ), with curves illustrating the trajectories of the outer and inner front wheels as the vehicle changes direction. The axes of all wheels intersect at the center O to ensure the vehicle turns without lateral slip. The turning radius R is calculated from the vehicle's center to O as follows:

$$R = \frac{L}{\tan(\delta)} \tag{9}$$

Turning radii of the inner rear wheel (R_3) and outer rear wheel (R_4) are expressed as:

$$\begin{cases} R_3 = R - \dfrac{D}{2} = \dfrac{L}{\tan(\delta)} - \dfrac{D}{2} \\ R_4 = R + \dfrac{D}{2} = \dfrac{L}{\tan(\delta)} + \dfrac{D}{2} \end{cases} \tag{10}$$

Steering angle δ is assumed to be known in advance, ranging from 0° to 35°. In this study, to simplify the model for small, low-speed electric vehicles, the distance between the two front wheels is assumed to be equal to the distance between the two rear wheels**,** the steering angles of the individual front wheels are calculated as follows:

$$\begin{cases} \delta_1 = \arctan(\dfrac{L}{R_3}) \\ \delta_2 = \arctan(\dfrac{L}{R_4}) \end{cases} \tag{11}$$

By substituting Eq. (10) into e Eq. (11), we obtain

$$\begin{cases} \delta_1 = \arctan\left(\dfrac{L\sin(\delta)}{L - \dfrac{D}{2}\sin(\delta)}\right) \\ \delta_2 = \arctan\left(\dfrac{L\sin(\delta)}{L + \dfrac{D}{2}\sin(\delta)}\right) \end{cases} \tag{12}$$

The turning radii of the inner front wheel (R_1) and the outer front wheel (R_2) are calculated as Eq. (13):

$$\begin{cases} R_1 = \dfrac{L}{\sin(\delta_1)} \\ R_2 = \dfrac{L}{\sin(\delta_2)} \end{cases} \quad (13)$$

When rotating an instantaneous center O, the entire vehicle including wheels, the chassis, and others are considered a single rigid body. During rotating, all points on the rigid body shares the same angular velocity (ω), including the wheels, regardless of their distance from the center of rotation. The velocities of the inner front wheel (V_1), outer front wheel (V_2), inner rear wheel (V_3), and outer rear wheel (V_4) are calculated as Eq. (14):

$$\begin{cases} V_1 = \omega R_1 = V\dfrac{R_1}{R} \\ V_2 = \omega R_2 = V\dfrac{R_2}{R} \\ V_3 = \omega R_3 = V\dfrac{R_3}{R} \\ V_4 = \omega R_4 = V\dfrac{R_4}{R} \end{cases} \quad (14)$$

The study did not take into account steering dynamics and control; The steering angle is assumed to be known and used as an input to calculate wheel speed according to the Ackermann model.

3. Simulation and Experiment

The independent all-wheel drive system for electric vehicles is simulated as illustrated in Figure 3, consisting of four independent control rings. The set speed is calculated at the central speed controller (Figure 4) and transmitted to the BLDC motor control blocks, which are built on the model of Mahmud et al. [14], using a feedback signal from the Hall sensor. In this system, each wheel is controlled by a discrete PID controller deployed on the Arduino Mega 2560 microcontroller to ensure that the actual speed follows the set value. The PID controller calculates the speed deviation and adjusts the control signal sent to the BLDC driver according to the control laws show in Eq. (15):

$$G_{PID(z)} = K_p + K_i T_s \frac{1}{z-1} + K_d \frac{N}{1 + NT_s \dfrac{1}{z-1}} \quad (15)$$

The PID factors are calibrated using a trial-and-error method based on the stepping response of the 36 V – 350 W BLDC motor to achieve a stable response and small speed deviation.

Figure 5 shows us the motor load torque when the motor is working under two conditions. The first condition is when the vehicle is moving in a line at 15 km/h, which you can see in Figure 5(a). The second condition is when the vehicle is going up a slope of 5 degrees at 5 km/h, shown in Figure 5(b). At 15 km/h, the required load torque is 6.32 Nm, while the motor maintains an average torque of 6.38 Nm with a peak value of 21.01 Nm, indicating a sufficient torque reserve. During the 5° slope climbing condition, the required load torque increases to 13.62 Nm, and the average motor torque reaches 13.66 Nm, with a maximum value of 32.44 Nm, confirming adequate traction capability. Short-term negative and oscillatory torque observed in both cases is attributed to electromagnetic transients and does not affect the overall traction performance, as the average motor torque consistently exceeds the required load torque.

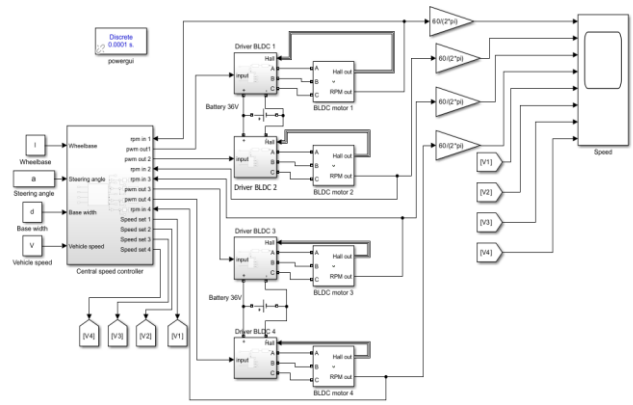

Figure 3. *PID control simulation of independent four-wheel drive system*

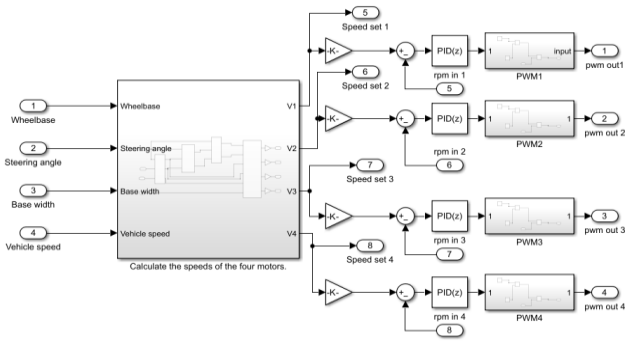

Figure 4. *Central speed controller*

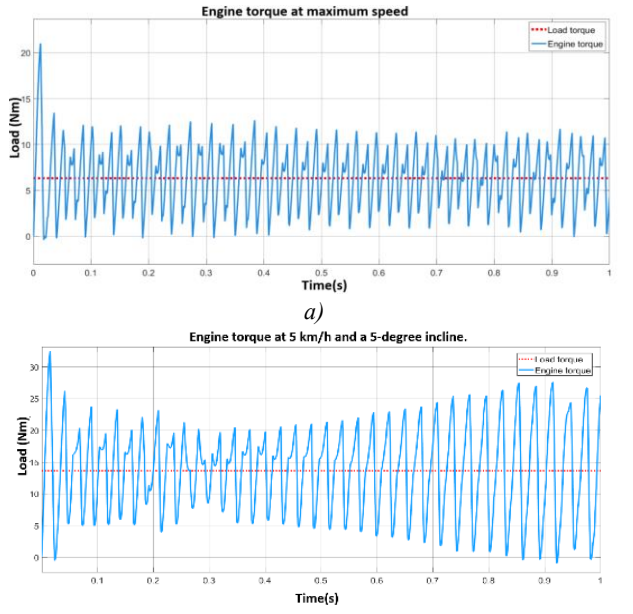

Figure 5. *Motor load torque simulation results*

a) Vehicles running at a maximum speed of up to 15 km/h on a straight line; b) Vehicles running at a speed of 5km/h and a slope of 5 degrees

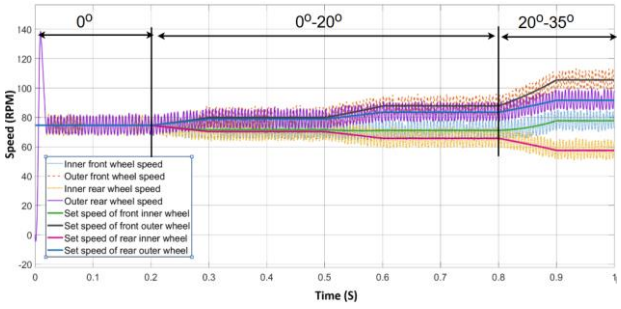

a)

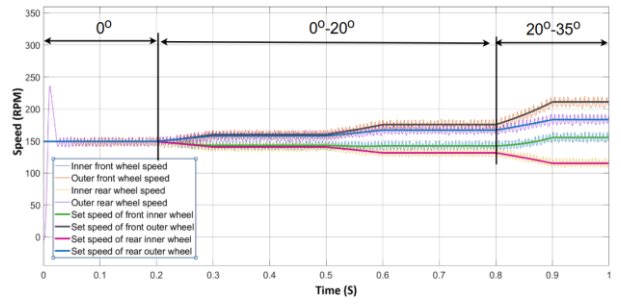

b)

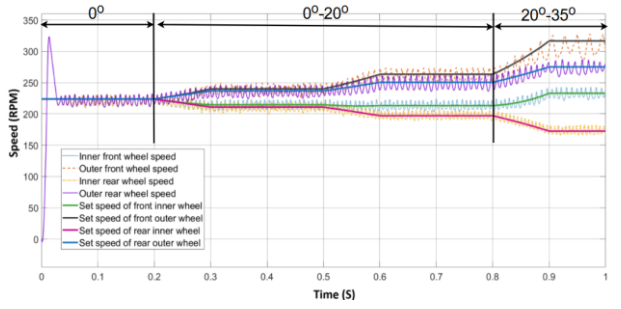

c)

Figure 6. *Simulates the rotation speed of four motors when the steering angle changes*

a) 5km/h; b) 10km/h; c) 15km/h

The independent four-wheel drive system is simulated at three speeds of 5 km/h, 10 km/h and 15 km/h with a driving angle that varies from 0°–35°. The simulation results in Figure 6 show that the PID controller maintains a stable speed of the wheels. During the straight travel phase, all four wheels adhere to the set speed, only a single large fluctuation appears when starting. When the steering angle increases from 0°–20°, the speed of the inner wheel decreases and the outer wheel increases according to the kinematic requirements, the control system responds well even though the setting speed changes quickly. In the 20°–35° zone, the amplitude varies more but the wheels keep up with the set speed without significant deviation.

After the elimination of the start-up phase, the system clearly demonstrates stability throughout the entire steering process. At 5 km/h (Figure 6(a)), the fluctuation is small (1–7 rpm) and the gripping speed is smooth. At 10 km/h (Figure 6(b)), the oscillation remains within 1–7 rpm and is frequently around 4.7–5.2 rpm. At 15 km/h (Figure 6(c)), the oscillation increases to 13–30 rpm and fluctuates frequently around 6.7–9.7 rpm, but remains within the permissible limits. These results show that the PID controller maintains effective traction at all three speed levels and under conditions of constantly changing steering angles.

To evaluate the feasibility of the model, a prototype electric vehicle was assembled, as shown in Figure 7(a). Figure 7(b) presents a general focus on the independent all-wheel drive system, making no mention of the steering system, steering angle sensors, or accelerator pedal sensors provided to the controller to regulate the rotational speed of the four independent motors. Speed of wheel based on hall signals were measured by a Hantek 6022BL device and exported data in Excel file. MATLAB was used for data processing and graphing and then compared with the simulation data.

a)

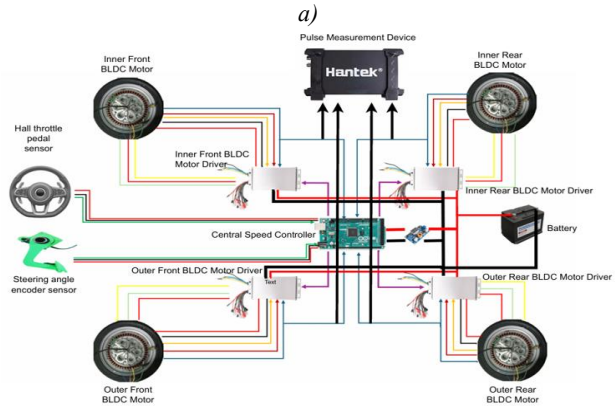

b)

Figure 7. *Structure of 4WD electric vehicle and control system schematic*

a) Structure of 4WD electric vehicle; b) Control system schematic

The experiment was carried out 5 times according to three set speeds of 5, 10 and 15 km/h, the steering angle was changed in three stages: 0°, 0–20° and 20–35°. The actual average speed values of the wheels are summarized in Table 2. When the car is driving straight, the measured average speed is very close to the set value, at 5 km/h it is 75.01–75.40 rpm compared to 75 rpm and at 10 km/h it is 148.83–149.40 rpm compared to 149 rpm. As the steering angles increase to 20° and 35°, the speed of the wheels changes in accordance with Ackermann's law, in which the inner wheel decreases and the outer wheel accelerates. Although the average speed of the wheels closely follows the set value, the instantaneous speed fluctuation of each wheel is still relatively large, which is evident from the measurement results represented in Figure 8.

Table 2. *Average speed of each motor 5 measurements*

Steering Angle	0°	20°	35°
5 km/h			
Set speed of rear inner wheel	75	66	58
Set speed of rear outer wheel	75	83	92
Set speed of front inner wheel	75	71	78
Set speed of front outer wheel	75	88	106
Inner rear wheel speed	75.40	65.73	57.70
Outer rear wheel speed	75.03	82.62	92.05
Inner front wheel speed	75.01	71.23	77.76
Outer front wheel speed	75.06	88.17	106.59
10km/h			
Set speed of rear inner wheel	149	131	115
Set speed of rear outer wheel	149	167	183
Set speed of front inner wheel	149	142	155
Set speed of front outer wheel	149	176	211
Inner rear wheel speed	149.40	130.37	114.87
Outer rear wheel speed	148.83	167.38	183.43
Inner front wheel speed	148.99	141.80	155.18
Outer front wheel speed	148.88	176.20	212.12
15km/h			
Set speed of rear inner wheel	224	197	173
Set speed of rear outer wheel	224	250	275
Set speed of front inner wheel	224	213	233
Set speed of front outer wheel	224	263	317
Inner rear wheel speed	223.96	196.75	172.14
Outer rear wheel speed	224.23	250.11	275.73
Inner front wheel speed	224.49	213.14	233.20
Outer front wheel speed	223.29	263.42	318.79

Figure 8 presents the experimental results at three velocity levels. At 5 km/h (Figure 8(a)), the speed of the wheels fluctuates greatly, especially during the transition from straight to turning, with an amplitude of about 20–30 rpm, but the trend still follows the set speed. As the velocity increases to 10 km/h (Figure 8(b)), the frequency of feedback from the Hall sensor increases, making the PID controller more stable, and the amplitude of the oscillation decreases to about 10–15 rpm. At 15 km/h (Figure 8(c)), the system works steadily, the speed of the wheels changes smoothly when turning, and the oscillation decreases.

Comparison with the simulation results in Figure 6 shows that the speed fluctuations in the experiment are significantly larger than in the simulation, especially in the low-velocity region. The main cause comes from the low resolution of the Hall sensor (26 pulses/cycle) combined with a sampling cycle of 500 ms, which reduces the speed measurement accuracy at low speeds and causes fluctuations in the PID control signal. Meanwhile, the simulation does not take into account sensor noise, measurement delays, and sampling limits, so it reflects more ideal conditions. As the speed of the vehicle increased, the measurement accuracy improved, making the experimental results at 10 km/h and 15 km/h close to the simulation. Although oscillations exist at low velocities, the trend of distributing speed between wheels during rotation is still consistent with the proposed kinematic model.

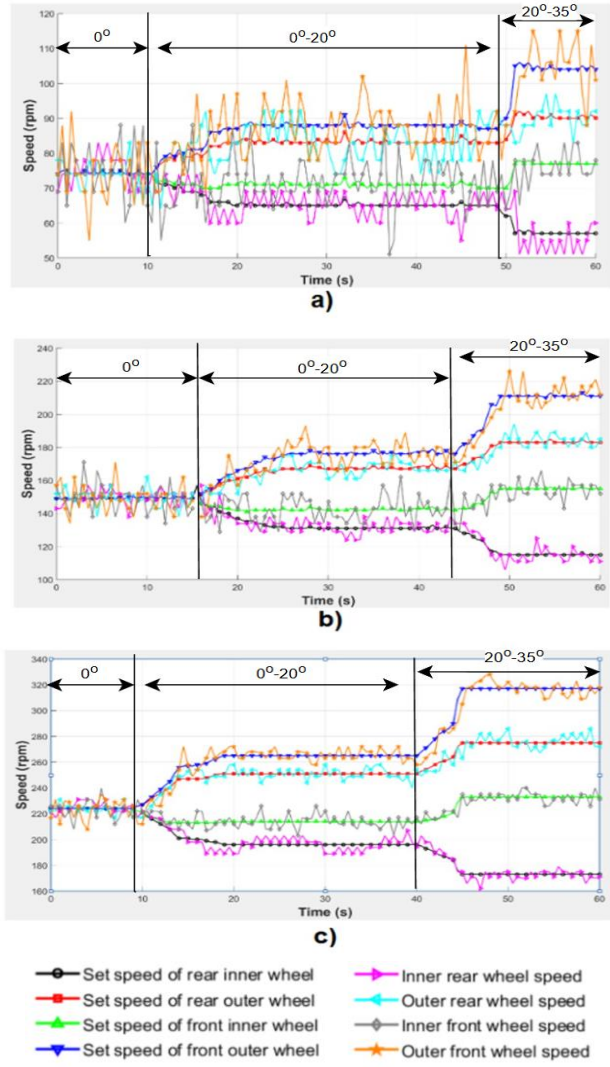

Figure 8. *Experimental results of the independent four-wheel drive system: a) 5km/h, b) 10km/h, c) 15km/h*

4. Conclusion

This study experimentally and numerically validates an independent all-wheel drive system for low-speed electric vehicles, in which each wheel is independently controlled based on the Ackermann kinematic model using 350 W in-wheel BLDC motors and PID controllers. Strategies for torque coordination control and high-level supervisory control for wheel slip control and dynamic stabilization under extreme operating conditions are beyond the scope of this study and will be considered in subsequent work. The experimental results show good agreement with simulation, particularly at medium and high speeds. Larger speed fluctuations are observed at low speeds due to the limited resolution of the Hall sensors (26 pulses/ revolution) and a 500 ms sampling period. Despite these limitations, the system achieves accurate wheel speed distribution and stable vehicle motion, while future improvements may be achieved through higher-resolution sensors, advanced control methods. The results confirm the feasibility of implementing simple PID control on low-cost hardware for low-speed electric vehicles.

List of symbols:

F_k	Traction force
F_i	Grade resistance
F	Rolling resistance
F_w	Aerodynamic drag
F_j	Inertial resistance
C_D	Aerodynamic drag coefficient
A	Frontal area of vehicle in square meters
v	Vehicle speed corresponding, km/h
m	Total vehicle mass
g	Gravitational acceleration
f_r	Rolling resistance coefficient
α	Road slope angle
σ	The rotational mass factor
$\frac{dv}{dt}$	The vehicle acceleration, m/s^2
P_{max}	Required power of the entire system
V_{max}	Maximum vehicle speed
ω	Angular velocity
P_{motor}	Power required for each motor
R	Calculated from the vehicle's center to O
R_1, R_2, R_3, R_4	Turning radii of inner front, outer front, inner rear, and outer rear wheel, respectively
V_1, V_2, V_3, V_4	Velocities of inner front, outer front, inner rear, and outer rear wheel, respectively
$\delta, \delta_1, \delta_2$	Vehicle's steering angle, steering angle of inner front, and outer front wheel, respectively
$G_{PID(z)}$	Transfer function of discrete PID controller
K_p	Proportional gain
K_i	Integral gain
K_d	Derivative gain
T_s	Sampling Cycle
z	Z Transform
N	Differential filter coefficient

REFERENCES

[1] S. Zhu and C. Lyu, *Distributed Drive Control Technology of Hub Motor. Singapore*: Springer Nature Singapore, 2025, doi: 10.1007/978-981-97-2922-7_1.

[2] M. Yıldırım, M. Polat, and H. Kurum, "A survey on comparison of electric motor types and drives used for electric vehicles*", in Proc. 16th Int. Power Electron. Motion Control Conf. Expo. (PEMC)*, 2014, pp. 218–223, doi: 10.1109/EPEPEMC.2014.6980715.

[3] M. S. Kumar and S. T. Revankar, "Development scheme and key technology of an electric vehicle: An overview", *Renewable Sustainable Energy Rev*, vol. 70, pp. 1266–1285, 2017, doi: 10.1016/j.rser.2016.12.027.

[4] M. Mahmud, M. R. Islam, S. M. A. Motakabber, M. D. A. Satter, K. E. Afroz, and A. K. M. A. Habib, "Control speed of BLDC motor using PID", *in Proc. 2022 IEEE 18th Int. Colloquium Signal Process. Appl. (CSPA),* 2022, pp. 150–154, doi: 10.1109/CSPA55076.2022.9782030.

[5] Z. Adel, A. A. Hamou, and S. Abdellatif, "Design of real-time PID tracking controller using Arduino Mega 2560 for a permanent magnet DC motor under real disturbances", *in Proc. 2018 Int. Conf. Electr. Sci. Technol. Maghreb (CISTEM),* 2018, pp. 1–5, doi: 10.1109/CISTEM.2018.8613560.

[6] H. Wang, "Design and implementation of brushless DC motor drive and control system", *Procedia Eng*, vol. 29, pp. 2219–2224, 2012, doi: 10.1016/j.proeng.2012.01.291.

[7] M. Mosin, N. Popov, V. Anibroev, M. Vilberger, and E. Domakhin, "Engine power distribution system for four-wheel drive autonomous electric vehicle", *Energy Reports*, vol. 9, Suppl. 1, pp. 115–122, 2023, doi: 10.1016/j.egyr.2022.10.388.

[8] K. Deepak, M. A. Frikha, Y. Benômar, M. El Baghdadi, and O. Hegazy, "In-wheel motor drive systems for electric vehicles: State of the art, challenges, and future trends", *Energies*, vol. 16, no. 7, Art. no. 3121, 2023, doi: 10.3390/en16073121

[9] O. Castro-Heredia, J. Linares-Flores, O.-D. Ramirez-Cardenas, G. Escobar-Valderrama, J. E. Valdez-Resendiz, and G. Curiel-Olivares, "Electronic differential speed control for a four in-wheel motors EV based on a multi-agent system", in *Proc. 2023 Int. Symp. Electromobility (ISEM)*, Monterrey, Mexico, 2023, pp. 1–7. doi: 10.1109/ISEM59023.2023.10334710.

[10] Z. Gmyrek, "Optimal electric motor designs of light electric vehicles: A review", *Energies*, vol. 17, no. 14, p. 3462, 2024, doi: 10.3390/en17143462.

[11] M. Yildirim and H. Kurum, "Electronic Differential System for an Electric Vehicle with Four In-wheel PMSM", *in Proc. IEEE 91st Vehicular Technol. Conf. (VTC2020-Spring),* Antwerp, Belgium, 2020, pp. 1–5, doi: 10.3390/en1714346.

[12] A. Vozmilov, L. Andreev, and S. Panishev, "The Development and Modeling of a Proportional Integral Controller for the Electronic Differential of an Electric Vehicle", *in Proc. 2022 Int. Conf. Ind. Eng., Appl. Manuf. (ICIEAM)*, Sochi, Russian Federation, 2022, pp. 578–582, doi: 10.1109/ICIEAM54945.2022.9787188.

[13] M. Yıldırım, E. Oksuztepe, and H. Kurum, "Design of Electronic Differential System for an Electric Vehicle with Four Independently Controlled In-Wheel PMSM", *Advances in Electrical and Computer Engineering,* vol. 24, no. 1, pp. 23–32, 2024, doi: 10.4316/AECE.2024.01003.

[14] M. Mahmud *et al*., "Control BLDC Motor Speed Using PID Controller", *Int. J. Adv. Comput. Sci. Appl.,* vol. 11, 2020, doi: 10.1109/CSPA55076.2022.9782030.